

EFFECT OF CROSS-SECTIONS DATA ON CALCULATED STATIC NEUTRONIC PARAMETERS OF PWR MOX/ UO_2 CORE TRANSIENT BENCHMARK CASE USING NODAL3 CODE

WAHID LUTHFI*, SURIAN PINEM

Research Center for Nuclear Reactor Technology, Research Organization for Nuclear Energy, National Research and Innovation Agency (BRIN), 80th Building Science and Technology Research Center (PUSPIPTEK), South Tangerang, Banten, Indonesia

* corresponding author: wahi004@brin.go.id

ABSTRACT. This paper describes the effect of cross-section data generated by several codes on calculated neutronic parameters. The Pressurized Water Reactor Mixed Oxide and Uranium Oxide (PWR MOX/ UO_2) Core Transient Benchmark case was chosen because it has been used widely to validate neutronic codes. The cross-section data in this study will be generated by SRAC, Serpent, and HELIOS codes. The NODAL3 code will be used to calculate neutronic parameters from each cross-section. The neutronic parameters calculated by NODAL3 are the effective multiplication factor (k_{eff}), control rod worth, critical boron concentration, and power distribution under Hot Zero Power (HZP) conditions. The Power-Weighted Error (PWE) and Error-Weighted Error (EWE), as a measure of the relative error in fuel assembly power, are less than 5%, indicating that the calculation is consistent with DeCART as a reference. The difference in calculated radial power peaking factor for all three cross-sections to reference data reaches 6.284% (G-3), 8.438% (G-3), and 10.998% (C-7), respectively, for SRAC, Serpent, and HELIOS. The axial power distribution calculated by NODAL3 at the top and bottom of the reactor core has a relative error that peaked at 16.60%, 13.86%, and 10.20%, respectively, for cross-sections provided by SRAC, Serpent, and HELIOS. Further improvements are needed for NODAL3 by applying various discontinuity factors to improve its performance.

KEYWORDS: PWR MOX/ UO_2 transient benchmark, cross-sections, neutronic parameter, NODAL3.

1. INTRODUCTION

To support the nuclear R&D program, especially nuclear power plants, several planned and continuous stages are needed. One of the most important things is to train experienced personnel that understands nuclear power plant technology. The NODAL3 code has been developed as in-house software for a safety analysis of Pressurized Water Reactors (PWR) and has been used in static and transient parameter calculations for various PWR reactors. As a coupled neutronic and thermal-hydraulic code, NODAL3 solves steady-state and time-dependent few-group neutron diffusion equations in 3-dimensional Cartesian geometry. NODAL3 code has been verified to determine static parameters of several cases related to Light Water Reactor (LWR) benchmarks, such as IAEA-2D, KOERBERG, BIBLIS, and IAEA-3D [1]. For transient calculations, the NODAL3 code has been used in OECD/NEA CRP PWR rod ejection cases [2–4]. The steady-state and transient verification results show good results when compared with reference data.

The NODAL3 code requires few-group constants from the core material, called cross-sections data. NODAL3 code requires cross-section data for fuels and other materials in the reactor core. The cross-section data play a very important role in obtaining accurate neutronic calculation results [5, 6]. To un-

derstand the effect of using different cross-section data on neutronic parameters, the PWR MOX/ UO_2 Core Transient Benchmark case was chosen to be evaluated [7]. The PWR MOX/ UO_2 Core Transient Benchmark case was issued by the Nuclear Science Committee of the OECD Nuclear Energy Agency (NEA) as reference data to verify the calculations of PWR core using MOX fuel [8–10]. In this case, the cross-section data generated by HELIOS were provided by Purdue University [11]. The cross-section data generated by Serpent were obtained from PWR MOX/ UO_2 Transient Benchmark Calculation using Monte Carlo Serpent 2 code and used by open-source Nodal Core Simulator ADPRES [12]. Apart from those two cross-sections, cross-section data generated with SRAC, using the collision probability method available by the PIJ module of SRAC for fuels and other non-fuel materials, were used [13].

In this study, only the static calculation of PWR MOX/ UO_2 Transient Benchmark case by OECD NEA, calculated using NODAL3 code with cross-sections data generated by SRAC (NODAL3-SRAC), Serpent (NODAL3-Serpent), and HELIOS (NODAL3-HELOS), was carried out. The calculated static neutronic parameters are the effective multiplication factor (k_{eff}), control rod worth, critical boron concentration, and assembly power at hot zero power (HZP) condition. The resulting neutronic

parameters will be compared with data provided by benchmark reports, i.e. EPISODE, calculated by Osaka University – Japan, and DeCART, calculated by SNU/KAERI – Republic of Korea [7].

2. METHODOLOGY

The reactor core used in this benchmark of PWR MOX/ UO_2 is based on a 3,565 MWth four-loop PWR power plant by Westinghouse. Fuel assemblies consist of an array of 17×17 lattices of rectangular fuel pin cells. Fuel assemblies have four different enrichments, UO_2 fuel assembly has 2 types of uranium enrichment, 4.2%, and 4.5% enrichment, and each has 104 IFBAs (Integral Fuel Burnable Absorber). Furthermore, the MOX fuel assembly named MOX 4.0% and MOX 4.3% has 24 WABA (Wet Annular Burnable Absorber) pins. The $\frac{1}{4}$ core configuration is shown in Figure 1. A complete description and data on the benchmark can be seen in the reference [7].

Neutronic parameters were carried out with NODAL3 for a quarter core ($\frac{1}{4}$ core) 3D model under Hot Zero Power (HZP) conditions with an inlet temperature of 560 K and an inlet pressure of 15.5 MPa. There are 193 fuel assemblies within the reactor including 53 control assemblies with an assembly pitch of 21.42 cm. The axial part of the reactor model is divided into 18 layers, 16 layers for the active core at a height of 22.86 cm (a total of 365.76 cm), and a layer for top and bottom axial reflectors at a height of 21.42 cm. Each fuel region was modelled to use a 2×2 node in a radial direction and a node in an axial direction. The core is then surrounded by radial-reflector assemblies with a height of 21.42 cm, containing a 2.52 cm thick baffle, and having a coolant with the same condition as the inlet coolant.

The cross-sections data (few-group constants) generated by SRAC2006 consist of a macroscopic cross-section of transport ($\sum tr$), absorption reaction ($\sum a$), produced neutron (ν), fission reaction ($\sum f$), and neutron scattering ($\sum s$), and are generated with the PIJ module. The PIJ was used to solve 2D transport using the collision probability method and PEACO was used for the resonance absorption calculation. The perfect reflection boundary condition has been applied for the outer surface and the B1 equation was used as a weight for homogenised cross-section generation. 107 energy groups from ENDF/B-VII.0 nuclear data library are then condensed into 2 energy groups, made up of 59 fast neutrons and 48 thermal neutrons. The diffusion coefficient was generated from an inverse transport cross-section. The calculation results with the PIJ module have been verified in the PWR core calculation and give good results compared to the reference [14, 15], hence the generated cross-section data can be used in this study. Besides the cross-section data generated with SRAC2006 [13], the cross-section data generated by Serpent [12] and HELIOS [7] in general, consist of similar few-group constants that have been calculated for different fuel temperatures,

	1	2	3	4	5	6	7	8	
A	U 4.2% (CR-D) 35.0	U 4.2% 0.15	U 4.2% (CR-A) 22.5	U 4.5% 0.15	U 4.5% (CR-SD) 37.5	M 4.3% 17.5	U 4.5% (CR-C) 0.15	U 4.2% 32.5	
B	U 4.2% 0.15	U 4.2% 17.5	U 4.5% 32.5	M 4.0% 22.5	U 4.2% 0.15	U 4.2% (CR-SB) 32.5	M 4.0% 0.15	U 4.5% 17.5	
C	U 4.2% (CR-A) 22.5	U 4.5% 32.5	U 4.2% (CR-C) 22.5	U 4.2% 0.15	U 4.2% 22.5	M 4.3% 17.5	U 4.5% (CR-B) 0.15	M 4.3% 35.0	
D	U 4.5% 0.15	M 4.0% 22.5	U 4.2% 0.15	M 4.0% 37.5	U 4.2% 0.15	U 4.5% (CR-SC) 20.0	M 4.3% 0.15	U 4.5% 20.0	
E	U 4.5% (CR-SD) 37.5	U 4.2% 0.15	U 4.2% 22.5	U 4.2% 0.15	U 4.2% (CR-D) 37.5	U 4.5% 0.15	U 4.2% (CR-SA) 17.5		
F	M 4.3% 17.5	U 4.2% (CR-SB) 32.5	M 4.3% 17.5	U 4.5% (CR-SC) 20.0	U 4.5% 0.15	M 4.3% 0.15	U 4.5% 32.5		
G	U 4.5% (CR-C) 0.15	M 4.0% 0.15	U 4.5% (CR-B) 0.15	M 4.3% 0.15	U 4.2% (CR-SA) 17.5	U 4.5% 32.5			Assembly Type CR Position Burnup (Gwd/t)
H	U 4.2% 32.5	U 4.5% 17.5	M 4.3% 35.0	U 4.5% 20.0					Fresh Once Burn Twice Burn

FIGURE 1. Quarter-core fuel configuration [7].

coolant density & temperature, soluble boron concentration, and control rod position, all at a selected fuel burnup condition except the non-fuel element.

Serpent 2 generated few-group constants by modelling each type of fuel assembly in 3D and setting a reflective boundary condition outside, so it could tally the required value to calculate the cross-sections and other group constants using Monte Carlo transport. Non-fuel elements, i.e. surrounding baffle and water reflector, were modelled by including nearby fuel elements so it could get a proper neutron flux for the tallying process, while ENDF/B-VI.8 was used as nuclear data library. HELIOS cross section provided by Purdue University [11] uses a transport lattice calculation to generate homogeneous cross-sections based on HELIOS v.1.8 libraries, which were generated from ENDF/B-VI and collapsed into a 2-group from 47-group neutron. DeCART, as a main heterogeneous solution, used a 47-group neutron based on HELIOS v.1.8 libraries, which have been transport-corrected by P0 scattering and subgroup method for the resonance region. Both few-group constants provided by HELIOS from Purdue university and Serpent 2 have the Assembly Discontinuity Factors (ADF), but since our NODAL3 is not developed to use ADF, this value is not used in the NODAL3 calculation.

3. RESULTS AND DISCUSSION

The total control rod worth and also effective multiplication factor (k_{eff}) for All control Rods Out (ARO) and All control Rods In (ARI) conditions are shown in Table 1 with the results of the DeCART code (heterogeneous solution) being used as the main reference. As part of power peaking factor, Power-Weighted Error (PWE) and Error-Weighted Error (EWE) are used to accurately describe the fuel assembly power errors in the calculation. They are defined by Equations (1) and (2), respectively, and the assembly power relative

Code	Total control rod worth [pcm]	ARO			ARI		
		k_{eff}	PWE	EWE	k_{eff}	PWE	EWE
Nodal solutions							
NODAL3-SRAC	6842	1.061790	2.73	3.73	0.989880	3.16	4.59
NODAL3-Serpent	6995	1.057631	1.52	2.21	0.984772	2.74	4.31
NODAL3-HELIOS	6915	1.063571	1.79	4.16	0.990700	3.41	4.60
EPISODE	6849	1.063640	0.96	1.64	0.991420	1.66	2.16
Heterogeneous solutions							
DeCART	6801	1.058520	ref	ref	0.987430	ref	ref

TABLE 1. Control rod worth and static parameters under ARO and ARI conditions.

error, e_i , is defined by Equation (3). In general, PWE can be considered as absolute error and EWE as RMS (root mean square) error.

$$PWE = \frac{\sum_i |e_i| ref_i}{\sum_i ref_i}, \tag{1}$$

$$EWE = \frac{\sum_i |e_i| |e_i|}{\sum_i |e_i|}, \tag{2}$$

$$e_i = \frac{calc_i - ref_i}{ref_i} \times 100. \tag{3}$$

In addition, calculation results are also compared with the EPISODE code, which uses the same nodal solution as NODAL3 Code and 2 group constants. DeCART basically uses MOC (Methods of Characteristic) using 47-group energy neutron data and the difference between control rod worth calculated with NODAL3-HELIOS from DeCART is 114 pcm. The calculated control rod worth from NODAL3-SRAC against the DeCART reference is 41 pcm, lower than the HELIOS cross-section, while the one from NODAL3-Serpent is the highest at 194 pcm. This difference is quite small for the control rod worth. The HELIOS cross-section gives the highest difference in k_{eff} for ARO and ARI at 505 pcm and 32 pcm, respectively. When comparing NODAL3 with EPISODE, the highest difference in control rod worth is 146 pcm for the cross-sections data from Serpent.

These results indicate that the NODAL3 code is still quite close when compared to nodal-solutions code like EPISODE. The PWE and EWE values for all three cross-sections in ARO and ARI conditions are still lower than 5%, so it can be said that they are quite close to the reference data from DeCART.

The calculated critical boron concentration, delayed neutron fraction, and assembly power are shown in Table 2. These data will be compared with DeCART code as the main reference and also EPISODE as a similar code to NODAL3 that uses nodal solutions. The highest difference between NODAL3 and DeCART calculations is 120 ppm when using data from Serpent. While the highest difference from EPISODE is 45 ppm when using data from Serpent. All these differences show that the NODAL3 code does not

Code	Critical boron conc. [pcm]	Delayed neutron fraction [pcm]	Assembly power error PWE	EWE
Nodal solutions				
NODAL3-SRAC	1342	579	2.45	4.18
NODAL3-Serpent	1385	579	2.09	4.58
NODAL3-HELIOS	1343	579	2.02	4.93
EPISODE	1340	579	1.05	3.42
Heterogeneous solutions				
DeCART	1265	–	ref	ref

TABLE 2. Critical boron concentration calculation and static parameters under HZP condition.

produce a significant difference in determining critical boron concentration for all three cross-section data. It can be seen that nodal solvers like EPISODE and our NODAL3 provide similar responses for calculating critical boron concentration since it was iterating nodal diffusion calculation to achieve critical conditions from interpolating each 2G group constant from 0 to 2000 ppm boron concentration. On the contrary, DeCART, which solves neutron transport using 47G MOC, has a higher fidelity on the neutron spectrum, especially when interacting with strong neutron absorbers like soluble boron within the coolant. The delayed neutron fraction values give identical results, with PWE and EWE still being lower than 5%, which makes this calculation closer to EPISODE results.

In general, all calculation results from EPISODE were closer to DeCART than NODAL3 calculations. This can be caused by the better spatial discretisation of EPISODE. EPISODE uses a multi-group nodal expansion method (NEM), same as NODAL3, and uses a 2G HELIOS cross-section provided by Purdue University, but EPISODE uses 16 nodes per fuel assembly in the radial direction rather than 4 as is the case of NODAL3. EPISODE also uses 20 axial regions for the active core region, instead of 16 regions used by NODAL3, even though both codes use a single region on a top and bottom of the axial reflector.

Code	Fuel Type		$\nu\Sigma_f$	Σ_{tr}	D	Σ_a	Σ_s	
							G# to 1	G# to 2
SRAC	UO ₂ 4.2 %	G1	6.71E-03	2.26E-01	1.47E+00	9.43E-03	1.98E-01	1.93E-02
		G2	1.19E-01	7.14E-01	4.67E-01	9.02E-02	7.66E-05	6.23E-01
	MOX 4.0 %	G1	7.82E-03	2.27E-01	1.47E+00	1.00E-02	2.00E-01	1.79E-02
		G2	2.06E-01	6.67E-01	5.00E-01	1.58E-01	1.45E-04	5.08E-01
	Reflector	G1	0.00E+00	1.76E-01	1.89E+00	3.83E-04	1.39E-01	3.69E-02
		G2	0.00E+00	1.14E+00	2.93E-01	2.69E-02	7.76E-06	1.11E+00
Serpent	UO ₂ 4.2 %	G1	7.55E-03	2.28E-01	1.46E+00	1.01E-02	5.09E-01	1.66E-02
		G2	1.53E-01	8.22E-01	4.06E-01	1.15E-01	2.08E-03	1.28E+00
	MOX 4.0 %	G1	8.28E-03	2.28E-01	1.46E+00	1.18E-02	5.01E-01	1.41E-02
		G2	3.66E-01	8.66E-01	3.85E-01	2.49E-01	4.19E-03	1.24E+00
	Reflector	G1	0.00E+00	2.52E-01	1.32E+00	2.29E-03	6.29E-01	2.84E-02
		G2	0.00E+00	1.33E+00	2.51E-01	3.80E-02	6.83E-04	1.98E+00
HELIOS	UO ₂ 4.2 %	G1	7.58E-03	2.36E-01	1.41E+00	1.00E-02	5.10E-01	1.63E-02
		G2	1.55E-01	8.35E-01	3.99E-01	1.15E-01	0.00E+00	1.28E+00
	MOX 4.0 %	G1	8.31E-03	2.36E-01	1.41E+00	1.17E-02	5.02E-01	1.39E-02
		G2	3.69E-01	8.65E-01	3.85E-01	2.51E-01	0.00E+00	1.25E+00
	Reflector	G1	0.00E+00	3.02E-01	1.10E+00	2.43E-03	6.40E-01	2.75E-02
		G2	0.00E+00	1.23E+00	2.72E-01	3.72E-02	0.00E+00	1.99E+00
Relative difference to HELIOS								
SRAC	UO ₂ 4.2 %	G1	-11.538 %	-4.035 %	4.204 %	-6.081 %	-61.266 %	18.602 %
		G2	-23.359 %	-14.520 %	16.987 %	-21.778 %	0.000 %	-51.272 %
	MOX 4.0 %	G1	-5.896 %	-3.535 %	3.665 %	-14.580 %	-60.276 %	28.786 %
		G2	-44.109 %	-22.983 %	29.841 %	-36.859 %	0.000 %	-59.241 %
	Reflector	G1	0.000 %	-41.592 %	71.210 %	-84.204 %	-78.283 %	34.149 %
		G2	0.000 %	-7.313 %	7.889 %	-27.804 %	0.000 %	-44.271 %
Serpent	UO ₂ 4.2 %	G1	-0.451 %	-3.345 %	3.460 %	0.301 %	-0.380 %	1.948 %
		G2	-0.997 %	-1.551 %	1.576 %	-0.338 %	0.000 %	0.031 %
	MOX 4.0 %	G1	-0.296 %	-3.159 %	3.262 %	1.030 %	-0.361 %	1.395 %
		G2	-0.826 %	0.052 %	-0.052 %	-0.516 %	0.000 %	-0.277 %
	Reflector	G1	0.000 %	-16.499 %	19.759 %	-5.602 %	-1.800 %	3.274 %
		G2	0.000 %	8.413 %	-7.760 %	1.968 %	0.000 %	-0.302 %

TABLE 3. Few-group constants of various components being used in PWR MOX/UO₂ core benchmark case.

Homogenised cross-section data or few-group constants for several fuel assembly types being used in PWR MOX/UO₂ core benchmark case generated by SRAC, Serpent, and HELIOS can be seen in Table 3. The selected fuel assembly type was UO₂ 4.2% and MOX 4.0%, all at 0.150 GWd t⁻¹, 900 K fuel temperature, 580 K moderator temperature (711.87 gr L⁻¹), and 1000 ppm boron concentration, while a non-fuel element, reflector, had the same properties as mentioned before. Comparing each group constant generated by SRAC and Serpent with HELIOS provided by Purdue University, it can be seen that the SRAC few-group constant is significantly different to HELIOS as compared to Serpent, which is closer to HELIOS. As additional information, the diffusion coefficient of Serpent and HELIOS are calculated manually for Table 3 by an inverse transport cross-section $\left(D_g = \frac{1}{3 \sum_{tr,g}}\right)$. The colour-coded relative difference was based on discrepancies in each neutron group and fuel type, which

could emphasise local differences in each group's constants.

The direct measurement (experiment) of axial and radial power density cannot be done inside the core, so it is necessary to make an accurate calculation when designing a reactor core. The local power density in the hottest fuel assembly needs to be estimated accurately to prevent fuel melt while the reactor is in operation. Local power density could be used to calculate the fuel temperature and coolant temperature in that position, and various studies focused on the calculation of the power peaking factor. Hence, the power peaking factor as a ratio of the highest power density at a given position to the average power density in the reactor core is also an important reactor operation and safety parameter.

The NODAL3 calculated results of radial power distribution or normalised radial power distribution with cross-section data generated by SRAC, Serpent, and HELIOS are shown in Table 4. DeCART code is

	1	2	3	4	5	6	7	8
A	0.385	0.847	0.542	1.510	1.296	1.160	0.496	0.293
	0.366	0.813	0.546	1.564	1.290	1.147	0.523	0.276
	0.362	0.856	0.554	1.536	1.309	1.176	0.531	0.281
	0.357	0.838	0.548	1.493	1.298	1.196	0.468	0.282
B	0.847	0.871	0.823	1.357	1.733	1.073	0.831	0.392
	0.813	0.817	0.778	1.340	1.822	1.048	0.806	0.373
	0.856	0.874	0.765	1.376	1.792	1.046	0.812	0.373
	0.838	0.861	0.754	1.360	1.770	1.066	0.832	0.361
C	0.547	0.778	0.647	1.612	1.630	1.324	0.591	0.307
	0.542	0.823	0.633	1.563	1.631	1.342	0.557	0.324
	0.555	0.765	0.664	1.576	1.612	1.350	0.600	0.321
	0.549	0.754	0.661	1.553	1.622	1.379	0.526	0.327
D	1.510	1.357	1.563	1.297	1.615	1.462	1.050	0.373
	1.565	1.341	1.612	1.262	1.666	1.441	1.032	0.363
	1.539	1.378	1.577	1.304	1.620	1.413	1.049	0.375
	1.494	1.361	1.554	1.306	1.619	1.440	1.085	0.352
E	1.291	1.823	1.631	1.666	0.643	1.395	0.822	
	1.296	1.733	1.631	1.615	0.633	1.367	0.824	
	1.312	1.796	1.615	1.622	0.671	1.367	0.836	
	1.299	1.771	1.623	1.620	0.682	1.378	0.838	
F	1.160	1.073	1.342	1.462	1.367	1.089	0.427	
	1.148	1.049	1.325	1.442	1.395	1.076	0.416	
	1.180	1.049	1.354	1.417	1.370	1.111	0.442	
	1.197	1.067	1.380	1.440	1.378	1.142	0.438	
G	0.496	0.831	0.557	1.050	0.824	0.427		
	0.525	0.807	0.592	1.033	0.823	0.417		
	0.534	0.817	0.604	1.055	0.839	0.439		
	0.469	0.833	0.527	1.086	0.839	0.439		
H	0.293	0.392	0.324	0.373				DeCART-Reference
	0.278	0.375	0.309	0.364				NODAL3-SRAC
	0.278	0.370	0.318	0.376				NODAL3-Serpent
	0.284	0.391	0.327	0.353				NODAL3-HELIOS

TABLE 4. Normalised radial power distribution by NODAL3 using cross-section from SRAC, Serpent, and HELIOS.

used as reference data for radial power distribution. Table 4 shows that each fuel assembly normalised power has a similar trend to the DeCART reference data, with the power peaking factor or the highest power density being about 1.73-1.83 at the positions E2 and B5.

Table 5 shows the relative errors of normalised power in Table 4 to the reference DeCART values. It can be observed that the relative error of NODAL3 with the cross-section generated by SRAC is low in comparison to Serpent and HELIOS in terms of the highest power error in a positive and negative direction. The SRAC cross-section gives 6.284% as the highest power distribution error when compared to DeCART which occurs in G-3, the Serpent cross-section gives the highest difference of 8.438% at G-3, and the HELIOS cross-section from Purdue University maxes out at 10.998% at position C-7. All cross-section data show a similar trend in which the power distribution

tends to deviate from the DeCART reference on the peripheral side of the reactor where it is close to the radial reflector, which has a vacuum outer boundary condition. Errors also appear in positions close to the middle of the reactor where reflective boundary conditions have been applied since NODAL3 uses a quarter-core ($\frac{1}{4}$ core) model, as can be seen in Table 5.

It can be seen that the calculated results of the radial power distribution from the NODAL3 code with different cross-sections generated with different codes do not show a significant difference in terms of the total value. The difference in the normalised radial power distribution is due to the different methods and nuclear data used to generate few-group constants or cross-section data and the nuclear data library used, as SRAC uses ENDF/B-VII.0, Serpent uses ENDF/B-VI.8 and HELIOS v1.8 was based on ENDF/B-VI. Furthermore, all these results by NODAL3 show that NODAL3 needs to improve its solver when treating

	1	2	3	4	5	6	7	8
A	0.385	0.847	0.542	1.510	1.296	1.160	0.496	0.293
	-4.935 %	-4.014 %	0.738 %	3.576 %	-0.463 %	-1.121 %	5.444 %	-5.802 %
	-5.974 %	1.063 %	2.214 %	1.722 %	1.003 %	1.379 %	7.056 %	-4.096 %
	-7.273 %	-1.063 %	1.107 %	-1.126 %	0.154 %	3.103 %	-5.645 %	-3.754 %
B	0.847	0.871	0.823	1.357	1.733	1.073	0.831	0.392
	-4.014 %	-6.200 %	-5.468 %	-1.253 %	5.136 %	-2.330 %	-3.008 %	-4.847 %
	1.063 %	0.344 %	-7.047 %	1.400 %	3.405 %	-2.516 %	-2.286 %	-4.847 %
	-1.063 %	-1.148 %	-8.384 %	0.221 %	2.135 %	-0.652 %	0.120 %	-7.908 %
C	0.547	0.778	0.647	1.612	1.630	1.324	0.591	0.307
	-0.914 %	5.784 %	-2.164 %	-3.040 %	0.061 %	1.360 %	-5.753 %	5.537 %
	1.463 %	-1.671 %	2.628 %	-2.233 %	-1.104 %	1.964 %	1.523 %	4.560 %
	0.366 %	-3.085 %	2.164 %	-3.660 %	-0.491 %	4.154 %	-10.998 %	6.515 %
D	1.510	1.357	1.563	1.297	1.615	1.462	1.050	0.373
	3.642 %	-1.179 %	3.135 %	-2.699 %	3.158 %	-1.436 %	-1.714 %	-2.681 %
	1.921 %	1.548 %	0.896 %	0.540 %	0.310 %	-3.352 %	-0.095 %	0.536 %
	-1.060 %	0.295 %	-0.576 %	0.694 %	0.248 %	-1.505 %	3.333 %	-5.630 %
E	1.291	1.823	1.631	1.666	0.643	1.395	0.822	
	0.387 %	-4.937 %	0.000 %	-3.061 %	-1.555 %	-2.007 %	0.243 %	
	1.627 %	-1.481 %	-0.981 %	-2.641 %	4.355 %	-2.007 %	1.703 %	
	0.620 %	-2.852 %	-0.490 %	-2.761 %	6.065 %	-1.219 %	1.946 %	
F	1.160	1.073	1.342	1.462	1.367	1.089	0.427	
	-1.034 %	-2.237 %	-1.267 %	-1.368 %	2.048 %	-1.194 %	-2.576 %	
	1.724 %	-2.237 %	0.894 %	-3.078 %	0.219 %	2.020 %	3.513 %	
	3.190 %	-0.559 %	2.832 %	-1.505 %	0.805 %	4.867 %	2.576 %	
G	0.496	0.831	0.557	1.050	0.824	0.427		
	5.847 %	-2.888 %	6.284 %	-1.619 %	-0.121 %	-2.342 %		
	7.661 %	-1.685 %	8.438 %	0.476 %	1.820 %	2.810 %		
	-5.444 %	0.241 %	-5.386 %	3.429 %	1.820 %	2.810 %		
H	0.293	0.392	0.324	0.373				
	-5.119 %	-4.337 %	-4.630 %	-2.413 %				
	-5.119 %	-5.612 %	-1.852 %	0.804 %				
	-3.072 %	-0.255 %	0.926 %	-5.362 %				
								DeCART-Reference
								% Error NODAL3-SRAC
								% Error NODAL3-Serpent
								% Error NODAL3-HELIOS

TABLE 5. Relative error to reference DeCART values for calculated normalised radial power distribution by NODAL3 using cross-section from SRAC, Serpent, and HELIOS.

neutron flux on the core peripherals that use specific boundary conditions.

The axial normalised power distribution or relative power to average axial power is shown in Figure 2, with the maximum calculated axial power from NODAL3-SRAC, NODAL-Serpent and NODAL-HELIOS being 1.4967, 1.4850, and 1.4964, respectively, while the value for DeCART is 1.50. Since the axial power distribution from DeCART is only shown as a figure, we use a plot digitiser [16] to obtain the exact calculated value from DeCART axial power distribution plot. Therefore, the difference in the axial power peaking factor is shown in Figure 2 and it is peaking on the top and bottom core which is up to 16.60 % for NODAL3-SRAC, followed by 13.86 % for NODAL3-Serpent, and 10.20 % for NODAL3-HELIOS. These findings are higher than the power distribution deviation of the radial power

peaking factor, and this indicates that radial and axial power profiles are sensitive to the cross-section data and it could be caused by the absence of a discontinuity factor in NODAL3 to improve neutron balance in the diffusion calculation, especially on the core peripherals (radial and axial).

4. CONCLUSION

The effect of the cross-section data set on calculating static neutronic parameters for the case of MOX/ UO_2 Core Transient Benchmark has been carried out with the NODAL3 code. Cross-section data used in this study are from SRAC, Serpent, and HELIOS. The largest difference in k_{eff} value for All control Rods Out (ARO) and All control Rods In (ARI) is 505 pcm and 32 pcm, respectively, when using cross-section data from HELIOS. The largest difference in control rod worth from reference data is 194 pcm when

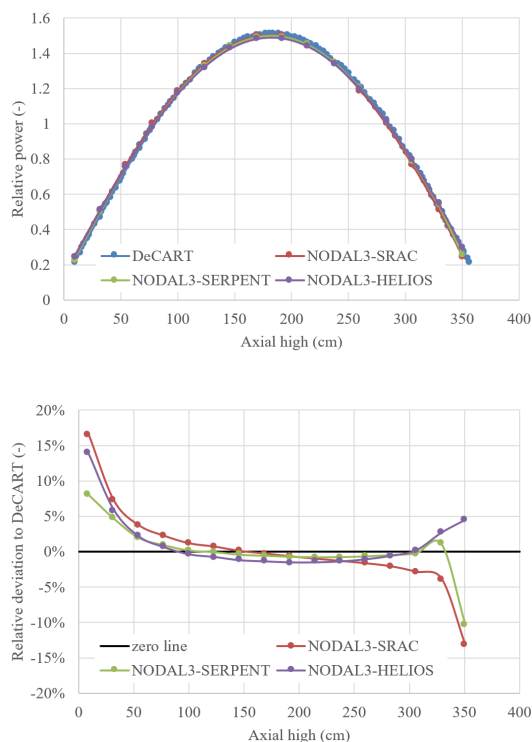


FIGURE 2. Axial relative power distribution and relative deviation to DeCart at HZP condition.

using cross-section data from Serpent, followed by the largest difference in the calculated critical boron concentration, 120 ppm, also from Serpent's cross-sections data. The relative errors in the fuel assembly power in both ARO and ARI conditions are still lower than 5%, while the difference in the calculated radial power peaking factor for all three cross-sections to reference data reaches 6.284% (G-3), 8.438% (G-3), and 10.998% (C-7) for SRAC, Serpent, and HELIOS, respectively. The calculated axial power distribution by NODAL3 has a relative error at the top and bottom of the reactor core that was peaking at 16.60%, 13.86%, and 10.20% for few-group cross-sections provided by SRAC, Serpent, and HELIOS, respectively. In conclusion, the 2-group cross-sections calculated by SRAC, SERPENT, and HELIOS were consistent with each other when the static parameters were calculated using NODAL3. Further improvements are needed for NODAL3 by applying various discontinuity factors to improve the neutron balance at reflective boundary conditions and in the peripheral zone of the reactor core near the radial and axial reflectors. In addition, another recommendation might be to manually upgrade or correct macroscopic cross-section data with an assembly discontinuity factor at each fuel assembly position inside the core before it is used as NODAL3 input.

ACKNOWLEDGEMENTS

We would like to express our gratitude to the Head of the Research Center for Nuclear Reactor Technology (PRTRN)

as well as the staff of the Nuclear Reactor Physics and Design Research Group, for their cooperation. The authors would like to say thank you to Donny Hartanto from Sharjah University for his help in generating the cross-sections and additional data needed for the calculations.

REFERENCES

- [1] T. M. Sembiring, S. Pinem. The validation of the NODAL3 code for static cases of the PWR benchmark core. *Jurnal IPTEK Nuklir Ganendra* **15**(2):82–92, 2012.
- [2] S. Pinem, T. M. Sembiring, P. H. Liem. The verification of coupled neutronics thermal-hydraulics code NODAL3 in the PWR rod ejection benchmark. *Science and Technology of Nuclear Installations* **2014**:845832, 2014. <https://doi.org/10.1155/2014/845832>
- [3] S. Pinem, T. M. Sembiring, P. H. Liem. NODAL3 sensitivity analysis for NEACRP 3D LWR core transient benchmark (PWR). *Science and Technology of Nuclear Installations* **2016**:7538681, 2016. <https://doi.org/10.1155/2016/7538681>
- [4] T. M. Sembiring, S. Pinem, P. H. Liem. Analysis of NEA-NSC PWR uncontrolled control rod withdrawal at zero power benchmark cases with NODAL3 code. *Science and Technology of Nuclear Installations* **2017**:5151890, 2017. <https://doi.org/10.1155/2017/5151890>
- [5] S. M. Reda, I. M. Gomaa, I. I. Bashter, E. A. Amin. Effect of MOX fuel and the ENDF/B-VIII on the AP1000 neutronics parameters calculation by using MCNP6. *Nuclear Technology and Radiation Protection* **34**(4):325–335, 2019. <https://doi.org/10.2298/NTRP190705002R>
- [6] T. Sakai, T. Yamamoto. Neutron cross section sensitivity analysis of UO₂ and MOX core physics experiments on light water reactors. *Journal of Nuclear Science and Technology* **51**(2):240–250, 2014. <https://doi.org/10.1080/00223131.2013.856774>
- [7] T. Kozłowski, T. J. Downar. PWR MOX/UO₂ core transient benchmark – final report. NEA/NSC/DOC(2006)20, Nuclear Energy Agency Organization for Economic Co-operation and Development, 70 pp., 2006, https://www.oecd-nea.org/science/wprs/MOX-UOX-transients/benchmark_documents/final_report/mox-uo2-bench.pdf.
- [8] J. Choe, S. Choi, P. Zhang, et al. Verification and validation of STREAM/RAST-K for PWR analysis. *Nuclear Engineering and Technology* **51**(2):356–368, 2019. <https://doi.org/10.1016/j.net.2018.10.004>
- [9] W. Luthfi, S. Pinem. Calculation of 2-dimensional PWR MOX/UO₂ core benchmark OECD NEA 6048 with SRAC code. *Tri Dasa Mega Jurnal Teknologi Reaktor Nuklir* **22**(3):89–96, 2020. <https://doi.org/10.17146/tdm.2020.22.3.5955>
- [10] M. Pecchia, G. Kotev, C. Parisi, F. D'Auria. MOX benchmark calculations by deterministic and Monte Carlo codes. *Nuclear Engineering and Design* **246**:63–68, 2012. <https://doi.org/10.1016/j.nucengdes.2011.10.005>
- [11] Purdue University. OECD/NEA and U.S. NRC PWR MOX/UO₂ core transient benchmark. 2004, [2020-07-07], https://engineering.purdue.edu/PARCS/MOX_Benchmark.

- [12] M. Imron, D. Hartanto. Pressurized water reactor mixed Oxide/ UO_2 transient benchmark calculations using Monte Carlo Serpent 2 code and open nodal core simulator ADPRES. *Journal of Nuclear Engineering and Radiation Science* **7**(3):031603, 2021. <https://doi.org/10.1115/1.4048764>
- [13] K. Okumura, T. Kugo, K. Kaneko, K. Tsuchihashi. SRAC2006: A comprehensive neutronics calculation code system. Tokai: JAEA, pp. 44–64, Japan, 2007. <https://doi.org/10.11484/jaea-data-code-2007-004>
- [14] S. Pinem, T. M. Sembiring, T. Surbakti, et al. Reactivity coefficient calculation for AP1000 reactor using the NODAL3 code. *Journal of Physics: Conference Series* **962**:012057, 2018. <https://doi.org/10.1088/1742-6596/962/1/012057>
- [15] S. Pinem, T. M. Sembiring, T. Surbakti. PWR fuel macroscopic cross section analysis for calculation core fuel management benchmark. *Journal of Physics: Conference Series* **1198**:022065, 2019. <https://doi.org/10.1088/1742-6596/1198/2/022065>
- [16] A. Rohatgi. WebPlotDigitizer version 4.6. 2022, [2023-05-02], <https://automeris.io/WebPlotDigitizer>.